Effect of Thermal Hydrolysis Pretreatment on Anaerobic Digestion of Protein-Rich Biowaste: Process Performance and Microbial Community Structures Shift

Jingyang Shi[1†], Guangyi Zhang[2,3*†], Hang Zhang[4], Fa Qiao[1,3], Jie Fan[4], Dingrong Bai[1] and Guangwen Xu[1]

[1]School of Chemical Engineering, Shenyang University of Chemical Technology, Shenyang, China, [2]School of Ecology and Environment, Beijing Technology and Business University, Beijing, China, [3]State Key Laboratory of Multiphase Complex Systems, Institute of Process Engineering, Chinese Academy of Sciences, Beijing, China, [4]School of Urban Construction, Wuhan University of Science and Technology, Wuhan, China

To reveal the effects of thermal hydrolysis (TH) pretreatment (THPT) on anaerobic digestion (AD) of protein-rich substrates, discarded tofu was chosen as the object, and its batch AD tests of tofu before and after being subjected to TH at gradually increasing organic loads were carried out and the AD process characteristics were compared; furthermore, its continuous AD tests without and with THPT were also conducted and the difference of the microbial community structures was investigated. The results showed that, during AD of protein-rich tofu with increase in the organic load, inhibition from severe acidification prior to accumulation of ammonia nitrogen (AN) occurred. THPT helped overcome the acidification inhibition present in batch AD of tofu at such a high TS content of 3.6%, to obtain the maximum methane yield rate of 589.39 ml·(gVS)$^{-1}$. Continuous AD of protein-rich tofu heavily depended on ammonia-tolerant hydrogenotrophic methanogens and bacteria. The continuous AD processes acclimated by HT substrates seemed to be resistant to severe organic loads, by boosting growth of ammonia-tolerant microorganisms, above all methylotrophic methanogens such as the genera RumEnM2 and methanomassiliicoccus. The process response of continuous AD of HT tofu was hysteretic, suggesting that a sufficiently long adaptation period was required for stabilizing the AD system.

Keywords: thermal hydrolysis, protein, tofu, anaerobic digestion, methanogenesis, microbial community structure

1 INTRODUCTION

In recent years, soybean protein, livestock, poultry breeding and dairy product, and meat product processing industries have been developing rapidly with the increasing demand for protein food all over the world, particularly in China with a large population. When bulky protein-rich food/feed are processed and consumed, large amounts of residual proteins have to be produced, including but not limited to tofu, minced meat, and other protein granules from food processing industries and home kitchens. Additionally, while more sewage treatment projects and pharmaceutical manufacturers are built and operated to meet the ever-increasing demand of human beings for a cleaner environment

and better medical care, large quantities of protein-rich sludges were produced, with their annual output surpassing 30 million tons per year (Mateo-Sagasta et al., 2015). These sludges mostly consist of extracellular polymer substances (EPSs), and various proteins take up an overwhelming proportion of EPSs (D'Abzac et al., 2010).

The above organic wastes and sludges are highly prone to corruption, especially since they are rich in proteins containing such heteroatoms as nitrogen and sulfur. Malodorous wastewater and gases often overflow during their degradation. If not handled properly, these protein-rich wastes and sludges will cause serious environmental pollution. However, on the other hand, protein is one of the three major nutritional components (the two others are carbohydrate and fat), and falls within a high nutritional biomass resource with better methane production potentials than carbohydrate (Nimas et al., 2017) and more rapid methane production rates than fat (Harris et al., 2017). From the protein-rich wastes and sludges, high calorific value biomethane can be obtained by AD, which will bring out significant environmental, economic, and social benefits.

AD refers to the process of decomposing organic matter and eventually generating methane and carbon dioxide through joint action of various microorganisms in the absence of oxygen (Ye et al., 2008). The AD process typically includes four stages: hydrolysis, acidification, acetogenesis, and methanogenesis (Appels et al., 2008). Each stage corresponds to specific microbial community, including hydrolytic acidification bacteria, hydrogen-producing acetogens, syntrophic acetate-oxidizing bacteria (SAOB), and methanogens (Tyagi et al., 2021). All kinds of microbes depend on and restrict each other in metabolic processes. As well known, there exist three main types of methanogens: acetotrophic, hydrogenotrophic, and methylotrophic, which support the three methanogenesis pathways, namely, acetoclastic, hydrogenotrophic, and methylotrophic methanogenesis, respectively.

To improve the AD efficiency for large particles and complex substrates, a variety of methods including physics (thermal) chemistry, physical chemistry, and biology are applied to pretreat the raw materials to change their biochemical properties. Among them, hydrothermal (HT) methods, also called thermal hydrolysis (TH) at high temperatures such as near the boiling point of water 100°C (Akiya and Savage, 2002; Kruse and Dinjus, 2007), which employs compressed high-temperature water (in liquid form) as medium to avoid the water gasification process, are highly favored because of the positive effect, low energy consumption, and environmental friendliness (Bougrier et al., 2008), especially suitable for biowastes with high water content (Kim et al., 2015), which has been successfully applied in large-scale engineering practice. It is commonly believed that high-temperature liquid water is conducive to the decomposition/degradation of protein particles and EPS into small particles and soluble substances and can thus lead to colloidal dispersion of sludge simultaneously, and can even excavate cellar walls to spill out nuclear materials under certain conditions, remarkably improving the biological accessibility and availability of the substrates. Moderately high temperature (120–160°C) TH is supposed to effectively accelerate

the degradation of big molecule proteins (Xue et al., 2015) and polysaccharide in organic matter and meanwhile restrict the nutrition loss caused by Mallard reactions and protein denaturation to an extent as low as possible (Lissens et al., 2004), to optimize the biogas production. The biogas yield was enhanced to $0.55\ L\cdot(gVS)^{-1}$ (Li et al., 2017) through thermal hydrolysis pretreatment (THPT) of municipal wastes rich in proteins. After treating antibiotic mycelial residue by THPT in combination with AD, Zhang et al. (2015) found that THPT completely eliminated the inhibition effect of antibiotics left in the antibiotic mycelial residue on the AD process and resulted in the methane yield rocketing up to $200\ ml\cdot(gVS)^{-1}$.

Generally, high protein content substrates are prone to release excessive amounts of AN in the process of AD due to their low C/N ratios, which can hinder methanogenesis to thus decrease the biogas yield and even destroy AD processes to cause AD system collapse (Resch et al., 2011). According to many studies (Calli et al., 2005; Han et al., 2015), some methanogens, mainly hydrogenotrophic and methylotrophic ones, can get certain amounts of AN accumulated in various substrates including protein-rich ones, but the balance of the main methanogenic pathways may change. Therefore, it is necessary and important to study the response of the AD system to excessive AN as well as the mitigation measures to the possible inhibition. After all, it is necessary for some protein-rich substrates to be subjected to THPT, e.g., for municipal sludge containing protein granule substrate and high protein content EPSs to enhance their biochemical properties (Villamil et al., 2020), and for (several million tons of) antibiotic mycelial residues to eliminate inhibition of antibiotics left in them (Zhang et al., 2015). That is, it is still essential to develop the technology of THPT combined with AD for the specific biowaste potential for biogas production. Anyhow, THPT has to result in changes of the compositions in the substrates; for instance, their contained proteins are subjected to denaturation and/or hydrolysis into forming small organic acids and ammonia, which undoubtedly affects the AD processes (Ramsay and Pullammanappallil, 2001; Chukwu and Ismail, 2010). However, so far, there are few details on the performance of AD process of these plant protein-rich substrates after THPT. In this paper, a typical kind of plant protein—tofu—was chosen as the digestion material and was subjected to batch and continuous AD tests without and with THTP, to probe into the changes caused by THPT including the resulting shift of the microbial community structures.

Thanks to scientific research and technology advancement, high-throughput sequencing technologies are developed and enable the determination of relative abundance of anaerobic microbes, thus providing detailed information on microbial community structures (Zhu et al., 2014). In addition, viable microbes are supposed to reflect the actual interaction between the functional microbes and the actual change of methanogenic pathways (Venkiteshwaran et al., 2015), and fortunately, at present, the living microbes can be separated from the dead ones, i.e., by propidium monoazide (PMA) sheltering (Li et al., 2014; Dorn-In et al., 2019). These technologies will also be used here to aid this research.

TABLE 1 | Physical and chemical properties of test materials.

Parameter	Tofu	TH tofu	Inoculated sludge for tofu	Inoculated sludge for TH tofu
pH	7.0	6.8	7.1	7.0
SCOD (mg/L)	3,404	5,111	3,077	5,375
TAN (mg/L)	34.85	153.9	905	785
TS (%)	7.26	8.49	8.81	8.74
VS (%)	6.81	8.12	6.67	6.86
VS/TS	93.79	95.59	75.73	78.41
C (%)	54.28	58.86	43.61	44.34
N (%)	9.381	9.093	3.383	3.392
C/N	5.79	6.47	12.89	13.07

Note: SCOD, soluble chemical oxygen demand; TAN, total ammonia nitrogen; TS, total solid; VS, volatile solid.

2 MATERIALS AND METHODS

2.1 Material Preparation and Characterization

The tested raw substrate, discarded tofu (rich in plant protein), was collected from a free market of agricultural products in Beijing, China. The TH tofu in the digestion experiment refers to the tofu after being subjected to TH in a THPT device (see **Section 2.2**). The inoculated raw sludge was collected from the AD unit of a poultry breeding company in Fujian province, China, and was acclimated before inoculation. To perform inocula acclimation, 600 ml of raw sludge was firstly introduced in two 2-L conical flasks, respectively; subsequently, 20 ml of tofu and TH tofu were added to the conical flask at the first 6 days, and then gradually increasing amounts (20–35 ml) of tofu and TH tofu were used at the later 14 days, respectively (for acclimating the inocula for the tofu and the TH tofu). The acclimation lasted for 20 days. The physical and chemical properties of the substrates and inocula are given in **Table 1**. As presented in **Table 1**, the total ammonia nitrogen (TAN) and soluble chemical oxygen demand (SCOD) in the resulting solid sample increased after THPT. It is worth noting that a lower nitrogen content and a higher C/N ratio in the TH protein-rich tofu were mainly due to part of nitrogen entering the liquid phase as the form of AN (Wang et al., 2018), corresponding to the high TAN and SCOD contents in the liquid.
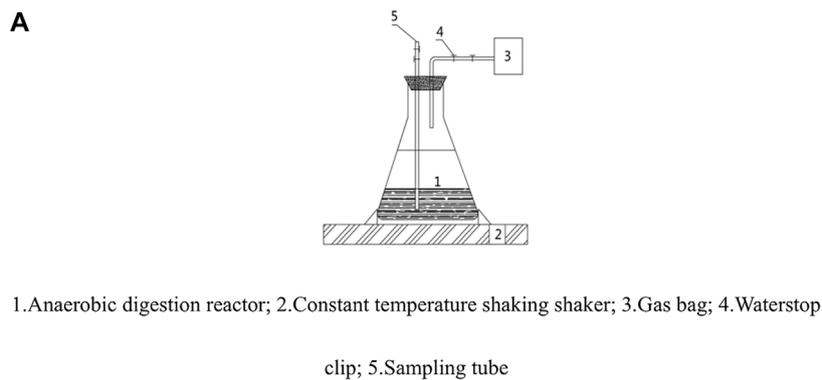
2.2 THPT

The THPT of tofu was carried out in a high-pressure reaction autoclave. The reaction autoclave is mainly composed of an internal autoclave body, a pressurized heating system, a cooling water circulating system, and a stirring system. The volume of the internal autoclave body is 1 L, the diameter is 70 mm, and a 1-L built-in steel vessel is equipped to hold the raw materials to be pretreated. The brief operation procedures are as follows: Firstly, 300 g of tofu and 500 ml of deionized water were measured out and mixed in a juicer to grind at a rotating speed of 12,000 RMP into tofu slurry. Then, 650 ml of tofu slurry was taken out and added into the steel vessel put in the reaction autoclave. Subsequently, after high-purity argon gas was introduced in the autoclave to purge for 5 min to drain the air
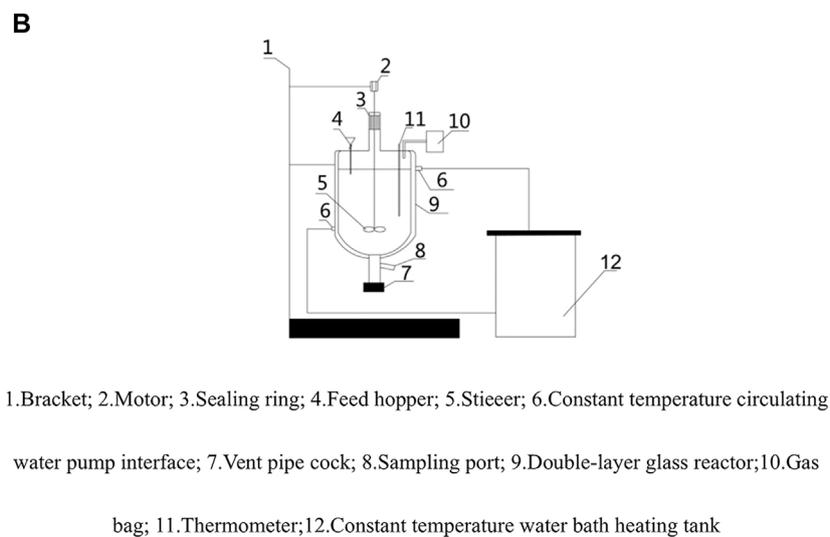
in the upper part of the autoclave, the heating system and stirring were open to heat the tofu slurry added in the steel vessel to a desired temperature for a preset duration. More details about the high-pressure reaction autoclave and the THPT operation procedures were described elsewhere (Zhang et al., 2014). In this research, the desired temperature for HTPT and the preset duration were chosen to be 120°C and 15 min, respectively, to ensure better AD performance and simultaneously minimize the nutrition loss of the protein-rich substrate caused by denaturalization and Maillard reaction and, after considering THPT at 140°C for 30 min, generate the maximum methane production for protein-rich antibiotic mycelial residue, but protein denaturation and Maillard reaction obviously happened (Liu et al., 2021a).

2.3 Batch AD

All the batch AD experiments with tofu before and after pretreatment were conducted through BMP tests. As shown in **Figure 1A**, the device for the BMP tests mostly consists of a constant temperature shaking incubator [preset at 37 (±1) °C] and several 680-ml conical flasks. Each conical flask was sealed with a rubber plug, through which one long and one short stainless-steel conduit with 4 mm inner diameter are installed. The short conduit was connected to a gas bag with a silica gel hose for collecting the produced gas, and the long one was used for sampling. Before the test, a vacuum pump was used to verify the air tightness of these conical flasks. The conical flasks were used as AD reactors with an effective volume of 600 ml. The BMP experiments were designed as **Table 2** shows. The mixture of the raw/TH tofu and the inocula were diluted with deionized water to obtain the target TS contents (1.2%, 2.4%, 3.6%, and 4.8%). Tofu and TH tofu were inoculated with the inocula accumulated using themselves, respectively. According to Boulanger et al. (2012), the maximum methane production rate and the minimal latency were reached at the inoculum/ waste (on volatile matter mass basis) ratio of 2 (when testing anaerobic degradation potential of municipal solid wastes). In addition, Zeng et al. (2010) observed that the maximum methane yield from anaerobic digestion of *Microcystis* spp. decreased when the inoculum/waste ratio decreased from 2.0 to 0.5. Therefore, for all the AD tests, the optimized substrate:inoculum ratio (based on VS) = 1:2 was chosen. Three parallel experiments were launched

A

1.Anaerobic digestion reactor; 2.Constant temperature shaking shaker; 3.Gas bag; 4.Waterstop

clip; 5.Sampling tube

The BMP device for batch AD

B

1.Bracket; 2.Motor; 3.Sealing ring; 4.Feed hopper; 5.Stieeer; 6.Constant temperature circulating

water pump interface; 7.Vent pipe cock; 8.Sampling port; 9.Double-layer glass reactor;10.Gas

bag; 11.Thermometer;12.Constant temperature water bath heating tank

The CSTR for continuous AD

FIGURE 1 | Diagrams of the experimental devices for **(A)** batch and **(B)** continuous AD. **(A)** The BMP device for batch AD and **(B)** the CSTR for continuous AD.

TABLE 2 | BMP test design for batch AD of tofu with different solid contents.

No	TS (%)	Condition	Substrate (g)	Seed sludge (g)	Water (g)
1	1.2	Untreated group	30	60	510
2	2.4		60	120	420
3	3.6		90	180	330
4	4.8		120	240	240
5	1.2	THPT group	25	58	517
6	2.4		50	116	434
7	3.6		75	174	351
8	4.8		100	232	268

simultaneously for each test. Once the inoculation in the conical flasks was completed, nitrogen was introduced to purge the air in the upper part of the conical flask for 10 min and the pH of the

substrate was adjusted to 7.0. Then, the conical flasks were placed on the table of the constant temperature shaking incubator to start the AD process, during AD intermittent shaking (shake for 30 min every 3 h at a speed of 120 RPM), until gas was no longer produced. When inhibition happened for batch AD of the raw tofu at 3.6% TS, 4 mol L^{-1} NaOH was used to adjust the pH to 7.0 (denoted as Raw 3.6%*).

2.4 Continuous AD

The continuous AD tests were carried out in several CSTR reactors. As **Figure 1B** depicts, the main body of each CSTR reactor was a double-layer glass reactor with an effective inner volume of 2 L, which was sealed with a rubber plug and wax. The temperature of the inner reactor for AD was controlled at 37°C (±0.5°C) by an outer water jacket connected to a circulating water bath. The material was fed by a glass funnel passing through the rubber plug. For each continuous AD test, on the first day, 1.2 L of

inoculum and 100 ml of tofu (or TH tofu) were added in the CSTR reactor and then a certain amount of deionized water was added as the balance to fill the inner reactor to 2 L. For the subsequent days, a certain volume of liquid digestate was discharged from the bottom of the inner reactor (before discharging, the liquid digestate was stirred to be homogeneous), and at the same time, an equivalent volume of substrate (tofu or TH tofu) was added (Test record: R, for raw tofu; R', for TH tofu). The performances of the continuous AD processes were recorded by monitoring and analyzing the daily parameters of the gas products and the liquid digestate, including gas yield and methane content (for gas product) as well as volatile fatty acids (VFAs) concentration, total ammonia nitrogen (TAN) concentration, pH, total solid content (TS), and volatile solid content (VS) (for the liquid digestate). At the first stages, the continuous AD processes for both raw tofu and TH tofu were operated at about 1.70 gVS·(L·d)$^{-1}$ organic load for 15 days; at the second stage, under about 1.91 gVS·(L·d)$^{-1}$ organic load for 30 days; and at the third stage, at about 2.34 gVS·(L·d)$^{-1}$ organic load for 30 days. In an exploratory experiments stage, the untreatment group was launched at an initial organic load of 2.1 gVS·(L·d)$^{-1}$, but acid inhibition took place and finally led to failure of the AD process.

2.5 Analysis Methods

The TS and VS of the liquid digestates were determined according to the national standard (Eaton, 2005). The pH value was measured with a pH meter (PE-20, METTLER TOLEDO Co., Ltd., Shanghai). TAN was analyzed by a portable rapid three-nitrogen detector (S-3N, Sinsche, Shenzhen), which was based on Nessler spectrophotometry. SCOD was measured by a rapid COD detector (CM-02), whose measurement principle was the potassium dichromate method. The elemental analysis was measured by an element analyzer [Vario Macro, Elementar Trading (Shanghai) Co., Ltd.], which was used to analyze the elemental content of organic solid samples (obtained after the high water content materials and the liquid digestate were dried). The volume of the gas product was determined by the draining saturated salt water method: A conical bottle was firstly filled with saturated salt water and then connected with a long tube and a short tube through its seal plug; when a certain amount of gas entered from the short tube into the conical bottle, the equivalent amount of liquid was discharged from the long tube, and finally, the volume of saturated salt water was measured by a volumetric cylinder and recorded as the volume of gas. The gas compositions of the gas products were analyzed by Agilent micro 3000 gas chromatography (Agilent micro 3000 GC, Agilent Technologies Inc., United States). To perform gas chromatography analysis, argon was used as the carrier gas, and the temperatures of injection port, column box, and detector were set to 100, 130, and 150°C, respectively, and the injection volume was 500 µl. The concentrations of VFAs were determined by an Agilent 7890A gas chromatograph (Agilent 7890A, Agilent Technologies Inc., United States). Nitrogen gas was used as the carrier gas, KB-FFAP capillary column was used for separation, and the FID detector was used for detection. The injection volume was 2 µl. The following programmed temperature was adopted for column

separation: the initial temperature was set at 80°C, then the temperature was increased to 130°C at the speed of 6°C·min^{-1}, and stayed at 130°C for 1 min and was finally increased to 220°C at 10°C·min^{-1}. During the process, the temperatures of the injection and the column were kept at 220°C; the temperature of the detector was also 240°C.

2.6 Illumina Sequencing and Data Analysis

Ten-milliliter liquid digestates on day 5, day 15, and day 75 were taken out, respectively, to represent the samples of the AD start-up, stable, and end stages. To recognize the viable microbes in the AD system, propidium monoazide (PMA) was use to process the liquid digestate samples to mask the dead ones in them. According to Dorn-In et al. (2019), to shelter the dead microbes in the samples, 1 mg of PMA was dissolved in 100 µl of dimethyl sulfoxide (DMSO) to make 20 mmol L^{-1} PMA pretreatment solution, which was immediately stored under shade and cooled at −20°C. Then, for each liquid digestate sample (500 µl), it was mixed with 2.5 µl of PMA pretreatment solution in a 1.5-ml centrifuge tube to ensure the actual concentration of PMA at 100 µmol L^{-1}. After violently shaken for 5 times, the mixture was then put under dark conditions to fully react for 5 min while the centrifuge tube was being continuously oscillated up and down. Finally, the centrifuge tube was placed on ice, and its cover was opened, and a 650-W halogen lamp was used to irradiate the mixture at a distance of 20 cm for 4 min. The samples on the 5th, 15th, and 75th day of the untreatment group were labeled as R1–3, and those of the THPT group were labeled as R'1–3, respectively.

From each PMA-pretreated sample, the DNA was extracted by MinkaGene Soil DNA Kit and its purity and concentration were detected by NanoDrop method (NanoDrop, Thermo Fisher Scientific, United States) using genomic DNA as the templates. To identify the diversity of bacteria, 16S rRNA gene V3–V4 was selected as the sequencing region, and 338F (5′-ACTCCTACG GAGGGCAGCA-3′) and 806R (5′-GGACTACHVGGTWT CTAAT-3′) were selected as the amplification intervals. To identify the archaeal diversity, 16S rRNA gene V4–V5 was selected as the sequencing region, and Arch519F (5′-CAGCCC CGCGGTAA-3′) and Arch915R (5′-GTGCTCCCCGCCAAT TCCT-3′) were selected as the amplification intervals. The prepared DNA samples were subjected to Illumina sequencing (using Illumina Hiseq 2500 platform, Guangdong Magigene Biotechnology Co., Ltd. Guangzhou, China). More detailed procedures about Illumina sequencing can be referred to elsewhere (Liu et al., 2020). The sequence data (deposited in the National Center for Biotechnology Information; BioProject ID: PRJNA779218, https://www.ncbi.nlm.nih.gov/bioproject/ PRJNA779218/) were transformed into Raw Reads by fastp software (version 0.14.1) through base recognition and analysis, and then spliced and filtered to get the Clean Tags (using usearch-fastq mergepairs V10 and fastp version 0.14.1). After clustering (at 97% identity) the Clean Tags into OTUs, the representative OTU sequences were selected to obtain species annotation information by comparison with the database (using usearch V10). The alpha diversity was calculated based on the normalized abundances [using QIIME software pack (V1.9.1)].
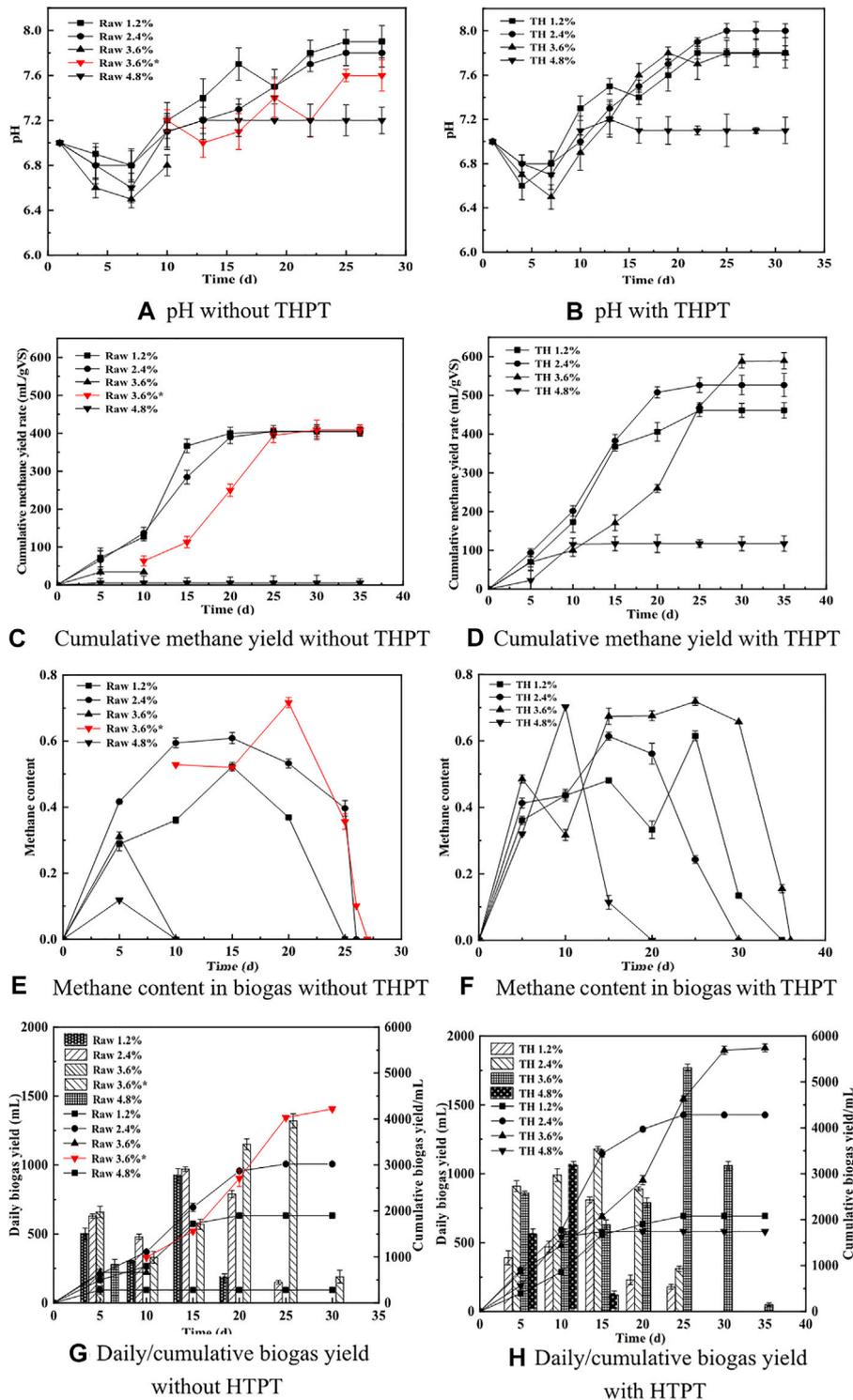
FIGURE 2 | Effects of THPT on the performances of batch AD of tofu. **(A** and **B)** The time-sequential changes of the pH value. **(C** and **D)** The cumulative methane yield. **(E** and **F)** The methane content in biogas. **(G** and **H)** The daily biogas/cumulative biogas yields, with and without THPT, respectively.

TABLE 3 | Process stability indicators after batch AD tests.

Parameters	Raw 1.2%	Raw 2.4%	Raw 3.6%	Raw 3.6%*	Raw 4.8%	TH 1.2%	TH 2.4%	TH 3.6%	TH 1.2%
pH	7.9	7.8	6.8	7.6	7.2	7.8	8.0	7.8	7.1
VFAs (mg/L)	776.58	2,575.55	5,989.79	1,052.81	7,569.11	3.97	35.06	932.44	7,165.59
Acetic acid	542.83	1,309.71	3,158.81	191.21	5,242.71	3.97	35.06	240.41	2,077.46
Propanoic acid	233.75	646.37	1,205.36	795.71	1,355.65	0	0	622.63	4,221.03
Isobutyric acid	0	401.52	1,098.01	36.72	664.92	0	0	37.04	487.64
Butyric acid	0	217.94	527.61	29.17	305.83	0	0	32.37	379.46
TAN (mg/L)	1,660	2,425	2,490	2,195	2,280	1,980	2,335	2,530	2,990
FAN (mg/L)	70.98	83.09	8.80	48.06	20.14	67.85	124.32	86.69	21.02
TS (mg/L)	2,600	5,567	8,267	8,433	11,078	4,483	9,417	7,298	10,424
VS (mg/L)	1933	3,167	6,450	8,167	8,022	3,233	6,550	5,671	8,317

Note: Raw/TH (1.2%, 2.4%, 3.6%, and 4.8%) respectively refer to batch AD, of tofu before and after being subjected to thermal hydrolysis (at 1.2%, 2.4%, 3.6%, and 4.8%).

3 RESULTS AND DISCUSSION

3.1 Performance of Batch AD of Tofu at Different TS Contents With and Without THPT

3.1.1 pH Change During Batch AD Without THPT
In the AD system, the decrease of pH is mainly affected by the activity of acidogenic microorganisms. As shown in **Figures 2A,B**, the pH change trend for each BMP experiment series was basically the same: decreasing at first, then increasing, and finally remained stable. This was closely related to the formation and consumption of VFAs (Chukwu and Ismail, 2010). At the initial stage of batch AD, the easy-to-degrade small-molecule organic matter in the substrates was rapidly hydrolyzed to produce VFAs (thus decreasing the pH value of the liquid digestate), and the pH reached its lowest level on the 7th day. However, as the AD proceeded, the VFAs were slowly decomposed/converted and assimilated, and meanwhile ammonia was generated and gradually accumulated. Finally, the pH value rapidly increased again, just because of the ammonia accumulation. Given the proper concentrations of VFAs providing sufficient substrates available for growth of microbes including methanogens, the substrates would, in turn, be consumed at accelerated rates by more microbes to produce a large amount of gas. As such, batch AD would proceed smoothly and the pH of the AD system became stable at the end of AD, when microbial growth and decay reached a balance. This assumption was true for tofu AD at low TS contents (1.2% and 2.4%). However, in the untreatment group with 3.6% TS content (Raw 3.6%), after 7 days of AD, the pH decreased to the lowest value of ca. 6.5, smaller than those for the untreatment groups with lower TS contents (1.2% and 2.4%). Though the pH gradually increased slightly within the subsequent 2 days, almost no gas was generated yet, indicating that the visible inhibition took place. This actually meant that "excessive" amounts of volatile acids were produced from hydrolysis of tofu but had not been digested quickly, resulting in severe acidification (refer to **Table 3** and **Section 3.1.2**) that hinders the activity of methanogens. Nevertheless, after the pH was adjusted to 7.2 with NaOH solution on the 8th day (Raw 3.6%*), the gas production was gradually restored. That is, alkali neutralizing the excessive VFAs could effectively relieve the acid inhibition of protein-rich substrate to realize stable AD operation at higher

loads (Zhang et al., 2019). In contrast, for the treatment group with the same TS content (TH 3.6%), throughout the whole digestion period, no obvious inhibition appeared, though on the 7th day, the pH reached the same lowest value (about 6.5) as the untreatment group. Instead, the pH gradually increased spontaneously and was finally stabilized. This was surely due to the excessive VFAs being metabolized by more methanogens adaptive to high acid concentrations (Franke-Whittle et al., 2014). Anyhow, when the TS increased to 4.8%, the pH was stabilized at pH = 7.1 earlier, despite the fact that its trend was consistent with those for other low TS groups, suggesting that the AD process was abnormal.

3.1.2 Effects of THPT on Methanogenic Characteristics
As **Figures 2C,D** show, the cumulative methane yield was visibly higher after THPT regardless of the TS content compared to the cases without THPT, although both the AD processes at the high TS content of 4.8% failed ultimately. Moreover, the higher the TS content, the higher the cumulative methane yield after THPT, except for the case with 4.8% TS content. Notably, at the same TS content of 3.6%, THPT helped smooth over the severe acidification (refer to **Sections 3.1.1** and **3.1.3**) occurring for AD of the raw tofu, to obtain the highest cumulative methane yield of up to 589.39 ml·(g VS)$^{-1}$ (TH 3.6%). For the latter, the AD process would not recover unless additional alkali was used. Even though alkali was added to overcome the acid inhibition during AD of the raw tofu with 3.6% TS content (Raw 3.6%), its cumulative methane yield tended to reach the same low values [410 ml·(g VS)$^{-1}$] as those for the lower TS contents (1.2% and 2.4%). These indeed exhibited the positive effects of THPT of protein-rich tofu on improving its nutrition for AD. As shown in **Figures 2E,F**, without inhibition happening (or after eliminating inhibition), the methane content in the biogas increased first, and then leveled off and finally plummeted for both the untreatment and treatment groups at all the TS contents. Presumably, at the initial stage of AD, methanogens were fully proliferated, generating biogas, above all methane, to increase the methane content in the biogas; then, the growth of methanogens slowed down and even stopped (due to lack of nutritious substrate at low organic loads or AD inhibition caused by high organic load), leading to steady biogas production with a relatively stable

methane content. Finally, at the late stage, with the continuous consumption of the substrates, biogas production dropped, and simultaneously methanogenesis gradually ended when the metabolism of methanogens themselves could not be maintained because of not enough nutritious substrate, which resulted in a sharp decrease in methane content in the biogas. After all, small amounts of other gases such as CO_2 and H_2 continued to be produced. The production of the gases was probably attributed to the release of small amounts of organic matter from microbes decaying at the endogenous respiration stage. Part of the organic matter was converted into CO_2 and H_2, with CO_2 dominating during hydrolytic acidification. When the produced gases are collected in gas bags and sampled every 1–3 days by removal from the AD systems for composition analysis, H_2 indeed blocked access to methanogens, further hindering methane generation. The mass transfer resistance of hydrogen between the syntrophic bacteria and methanogens was also put forward by Liu et al. (2021b). Here, it must be noted that the abovementioned gradual termination of methanogenesis at the late stage did not mean that there was no methane generated in biogas at all. In the untreatment group with 3.6% TS content (Raw 3.6%), the methane content peaked on the 20th day, reaching 71.65%, while in the treatment group with the same TS content (TH 3.6%), the equivalent maximum methane content appeared on the 25th day, later than that in the untreatment group. The methane content remained above 65% from the 15th to the 30th day in the treatment group. Such high methane contents remained for so long, suggesting that there existed more active methanogens, or the whole activity of methanogens was higher in the treatment group compared to the untreatment group with the same TS content.

Upon the premise that there was no inhibition appearing or the inhibition was eliminated (at TS contents of 3.6% or below), whether the substrate tofu was subjected to THPT or not, the cumulative biogas yield was basically proportional to the TS contents (that is, the amounts of substrates due to the fixed ratio of substrate: inoculum), while it was not true for the daily biogas yield, as given in **Figures 2G,H**. This actually verified the proliferation of microorganisms for the higher TS substrate at the initial stage of AD, consistent with the above presumption. Also, this well coincided with the phenomena that a lower cumulative methane yield was obtained for a higher TS content at the initial and middle stages (until the 20th day) of batch AD (see **Figures 2C,D**). Precisely because of the growth of highly adaptive methanogens, for TH tofu with a high TS content of 3.6%, there appeared accelerating increases in the cumulative biogas yield rate (**Figure 2H**), first being the cumulative methane yield rate (**Figure 2D**), during the middle and late stages (from the 20th to the 30th day), thus maintaining high methane contents of over 65% (see **Figure 2F**). This suggested that the AD system for digesting TH tofu took a relatively longer time to respond to change of organic load but performed better at last when compared to that for the raw tofu.

3.1.3 Stability Parameters
After each batch AD test, the stability parameters (final pH, VFAs, TAN, FAN, etc.) were measured and given in **Table 3**.

Keeping in mind that addition of alkali (NaOH) eliminated the inhibition present during AD of the raw tofu at 3.6% TS content, all the batch AD tests at TS content not higher than 3.6% proceeded smoothly, and the related parameter fell within their normal ranges [the threshold values for total VFAs, acetic acid, propanoic acid, TAN, and FAN are respectively 8,000 mg L^{-1}, 2,400 mg L^{-1}, 900 mg L^{-1}, 2,500–3,000 mg L^{-1}, and 185 mg L^{-1} (Hobson and Shaw, 1976; Massé et al., 2003; Siegert and Banks, 2005; Wang et al., 2009)]. For the untreatment group with 3.6% TS content (Raw 3.6%), the visible inhibition was observed on the 7th day, when the VFAs concentration reached up to 5,989.79 mg L^{-1}, and above all, the propanoic acid concentration was as high as 1,205.36 mg L^{-1}, far surpassing the threshold value of 900 mg L^{-1} 2 days later than when the inhibition took place, and the pH was adjusted to 7.2 by adding NaOH and the gas production gradually recovered and the methane content in the biogas reached over 50%. After 30 days of AD, the VFA concentration decreased to such a low value of 1,052.81 mg L^{-1} with the propanoic acid concentration (795.71 mg L^{-1}) being below its threshold value (900 mg L^{-1}). This indicated that accumulation of VFAs (first of all, propanoic acid) played a role in inhibiting the AD of tofu with heightening TS content, while considering that other parameters were far lower than their threshold values. However, for TH tofu with 3.6% TS content (TH 3.6), it continuously generated biogas, and the daily biogas yield rocketed up to ca. 470 ml on the 25th day (total volume of 1,800 ml from the 20th to the 25th day) after a latent period of 15–20 days. Throughout the whole AD process, all the related stability parameters were far away from their threshold values, stating that HTPT was effective to overcome acidification appearing in batch AD of modestly high TS content protein-rich substrates. While the worsening process of AD of 4.8% tofu was not reversed, HTPT still improved AD performance to some extent, particularly at the initial stage of AD. More methanogens adaptive to high acid and ammonia concentrations in the inoculum acclimated by HTPT of protein-rich tofu were supposed to be responsible. This was partially supported by the fact that the VFA concentration reached over 7,000 mg L^{-1} and the TAN concentration approached 3,000 mg L^{-1}. According to the results of several preliminary batch AD tests (not given here), it was found that AD of the raw tofu biogas production started to be slightly hindered when the AN concentration reached 2,500 mg/L. For both the untreatment and treatment groups with 4.8% TS content, gas production did not recover even after adjusting the pH to 7.0. The pH values of all the batch AD tests in the absence of inhibition were stable between 7.5 and 8.0, consistent with the previous research about protein-rich substrates (Yang et al., 2015).

3.2 Comparison of Continuous AD of Tofu With and Without THPT
3.2.1 Performance of Continuous AD and Effect of THPT
The performance of continuous AD of tofu before and after being subjected to THPT is illustrated in **Figures 3**, **4**. **Figure 3A** gives the daily biogas yield from continuous AD of tofu and the daily
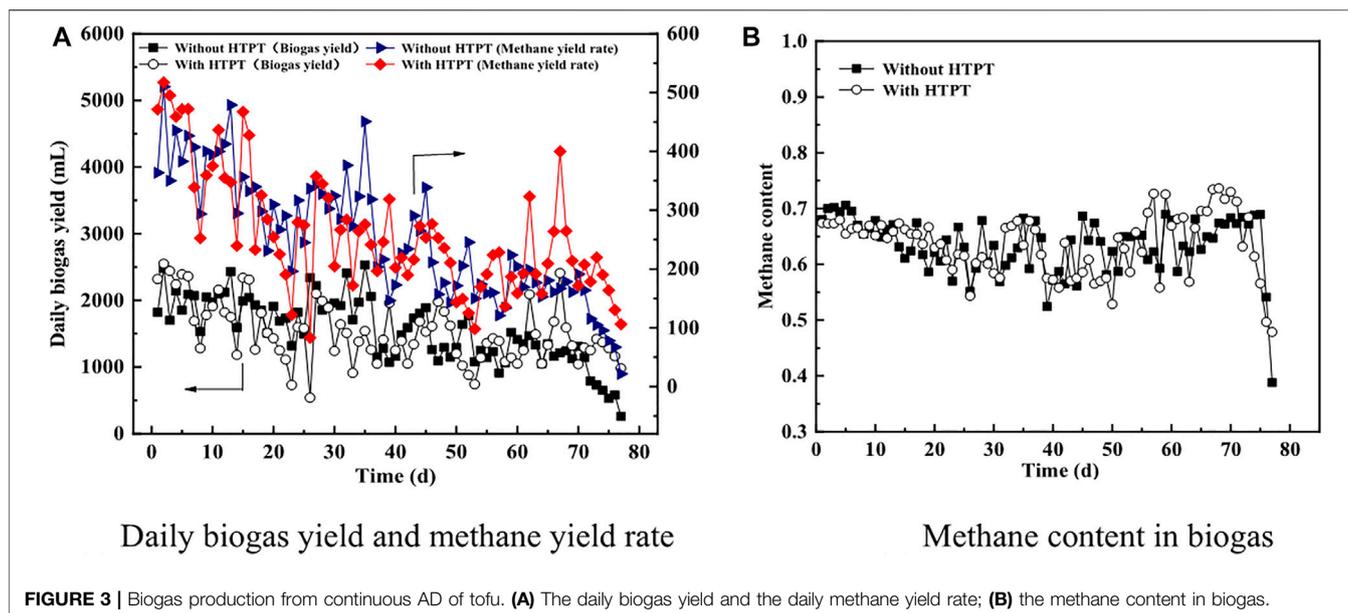
FIGURE 3 | Biogas production from continuous AD of tofu. **(A)** The daily biogas yield and the daily methane yield rate; **(B)** the methane content in biogas.

methane yield rate, and **Figure 3B** shows the methane content in biogas. It could be seen that at the first stage of AD with a low TS content [~1.70 gVS·(L·d)$^{-1}$], the average daily biogas yield for the treatment group (with THPT) is higher than that for the untreatment group (without THPT), when all the related indicators for AD were normal (including pH in **Figure 4A**, TAN and FAN in **Figures 4B,C**, respectively, and VFAs before and after HTPT in **Figures 4D,E**, respectively), signifying the smooth operation of continuous AD. This was also true for the daily methane yield rate [438 vs. 402 ml·(gVS)$^{-1}$] with the methane content in biogas basically unchanged. These results were consistent with those obtained from batch AD tests when there appeared no inhibition or after the inhibition was eliminated. However, at the second stage [the organic load was increased to 1.91 gVS·(L·d)$^{-1}$ from the 15th to the 45th day], the daily biogas yield and the daily methane yield rate for the treatment group was lower than those for the untreatment group, indicating the HTPT + AD system was sensitive to the organic load change. Compared to the first stage, though, the TAN and VFA concentrations were enhanced to certain extents for both the untreatment and treatment groups, and the amplifications were bigger for the treatment group than those for the untreatment group. This suggested that more protein in tofu was decomposed to small-molecule matter including lower fatty acids and ammonia (see VFAs in **Figure 4D** vs. **Figure 4E**; TAN with vs. without THPT in **Figure 4B**). Due to synchronous generation of lower fatty acids and ammonia, the pH value did not change obviously (**Figure 4A**). As a result, the FAN concentrations became slightly higher (**Figure 4C**) for the case with THPT, according to the relation of FAN with TAN and pH (Koster, 2010). Corresponding to less biogas production from TH tofu, the TS and VS contents of the liquid digestion were higher, in comparison with those from the raw tofu (without THPT) (see **Figures 4F,G**). Two possible reasons are as follows: (1) more organic particles were not digested and were left, and (2) more

microorganisms were generated (discussed hereinafter in **Section 3.3**). Parts of the residual organic particles and the generated microorganisms were discharged daily as wasted sludge, which were used for parametric analyses. As a matter of fact, the high concentrations of VFAs laid a good material base for growth of microorganism (first of all, bacteria, rather than methanogens, are more sensitive to environmental change). This was especially suitable for TH tofu (see **Figure 4E**). Except that for THPT-generated VFAs, proliferation of more active bacteria would, in turn, speed up decomposition of protein-rich tofu to produce additional VFAs, provided that the formed VFAs could not be assimilated and metabolized to complete extents. This synchronously led to formation of a large amount of ammonia, which well accorded with the higher TAN concentrations in the digestion liquid (**Figure 4B**).

When the organic load was increased to 2.34 gVS·(L·d)$^{-1}$ (the third stage of AD), the daily biogas yield and the daily methane yield rate further decreased for the untreatment group (without THPT) at the initial stage, while for the treatment group (with THPT), they did not take on a visibly decreasing trend but violently fluctuated. This indicated that the AD system acclimated by TH tofu was relatively more resistant to soaring organic load. Nevertheless, the two AD systems finally failed. However, insight into the changes of their process stability parameters revealed that the reasons for their failure differed distinctly from each other. For continuous AD of the raw tofu (without THPT), accumulation of VFAs happened prior to presence of excessively high TAN concentrations (see **Figures 4B,D**), which thus resulted in pH and FAN dropping (**Figures 4A,C**). This meant that VFA accumulation worsened the AD process right from the start. Notably, the concentration of propanoic acid was constantly higher than its threshold value (900 mg L^{-1}) for the untreatment group. In practice, accumulation of VFAs, first of all, propanoic acid, had been proven to be the first and primary inhibition factor during batch
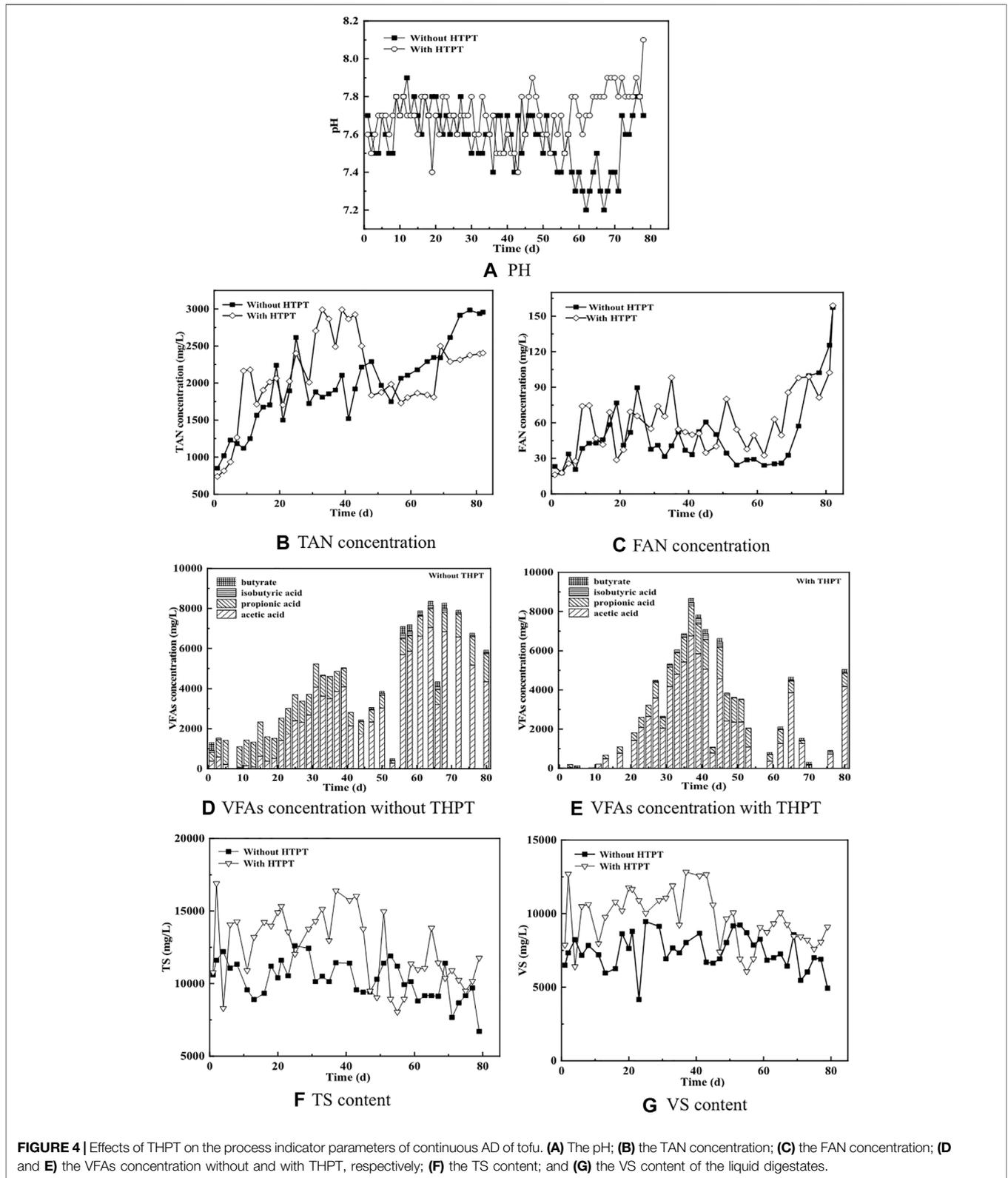
FIGURE 4 | Effects of THPT on the process indicator parameters of continuous AD of tofu. **(A)** The pH; **(B)** the TAN concentration; **(C)** the FAN concentration; **(D and E)** the VFAs concentration without and with THPT, respectively; **(F)** the TS content; and **(G)** the VS content of the liquid digestates.

AD of the raw tofu when performing batch AD tests of the raw tofu at a high TS content of 3.6%. To one's surprise, in spite of the fact that the continuous AD of the TH tofu (with HTPT) at the third stage also failed, all the process stability parameters fell within their normal ranges at the initial and middle stages. Just for this reason, it could easily be concluded that excessive amounts of

FAN, corresponding to the high pH value and the high FAN concentrations at the end of AD (shown in **Figures 4A,C**, respectively), took a duty-bound responsibility for the final failure for the treatment group (with THPT). Keeping this in mind, it could be reasonably inferred that discharging excessive amounts of high TS content liquid digestate at the second stage resulted in continuous AD of TH tofu finally failing at the end of the third stage, after taking into account that the TS and VS concentrations continue to drop from the end of the second stage. Accompanying blowoff of the liquid digestate, the active microorganisms, especially methanogens, were discharged but could not completely recover because of lower growth of most methanogens. Therefore, a longer acclimation period was necessary to stabilize the AD system of TH tofu after heightening organic load. Anyhow, a certain number of methanogens were left and played positive roles in maintaining the stability of AD by producing methane without interruption. This guaranteed that AD proceeded smoothly to continuously generate visible amounts of biogas, particularly methane (shown in **Figures 3A,B**), which accounted for the constantly highest methane contents for the AD system of the treatment group (with THPT) until the final failure at the end of the third stage (also shown in **Figure 3A**). Just before the final failure, the methane content in the biogas was maintained at ~70% for continuous AD of the HT tofu (with THPT) with its average value being invariably higher than that for the raw tofu (with THPT) (**Figure 3B**). The same phenomenon was also observed by other researches on substrate (Jia et al., 2017). Indeed, this implied that the methanogens left in the AD system acclimated by TH tofu were still highly active. At the condition that there were not enough methanogens present in the AD system, continuous high organic load led to excessively high contents of AN, particularly FAN. Therefore, the AD process finally collapsed.

It has been reported that, when the AN concentration exceeded $2,500 \, \mathrm{mg \, L^{-1}}$, the activity of methanogens tended to be inhibited, resulting in reduction of the total efficiency of the AD reactor, but the toxicity produced by inhibition had a certain lag (Kim and Kim, 2020). This actually explained the fact that for the treatment group (with THPT), there was no obvious inhibition when the TAN concentration reached the highest values (~$3,000 \, \mathrm{mg \, L^{-1}}$). Given that enough nutritious substrates (easier-to-metabolize small-molecule matter) were supplied from tofu after being HTPT, due to the accelerated growth of microorganisms, first of all, bacteria (rather than methanogens, discussed hereinafter in **Section 3.2.2**), part of AN was assimilated and the TAN concentration in the AD system dropped to far below its threshold value (shown **Figure 4B**). This led to restoration of AD microorganisms including methanogens to some extent at the end of the second stage, and thus relatively better AD performance occurred for the TH tofu (with THPT) at the first half of the third stage.

3.2.2 Analyses of Microbial Community Structure
(a) Sample bacterial sequencing results and alpha diversity analysis

Statistical results of sample sequencing data processing and alpha diversity indexes for continuous AD at various stages are given in **Table 4**. At the stable period, the clean total tags of both bacteria and archaea in samples from the treatment group (R′) were higher than those in the untreatment group (R), featuring a larger number of microorganisms present in the AD system for THPT. Each of the OTUs obtained at the similarity threshold of 97% after clustering analysis of Clean Total Tags of samples can correspond to a certain population of microorganisms, and the Chao1 index can reflect the richness of species. As seen from **Table 4**, at the start-up stage, both the average OTU number and Chao1 index of bacteria in R and R′ did not differ significantly from each other. However, at the stable period, both the average OTU number and the Chao1 index of bacteria in R′ were much higher than those in R, showing that after THPT, there were more bacterial populations and the bacterial species was richer. Simpson and Shannon indices were commonly used to reflect microbial community diversity. The Simpson diversity indices were lower, while the Shannon indices were higher for both bacteria and archaea in R, indicating their respective higher biodiversity. As a sequencing quality standard (the accuracy of each base is 99.9%), the Q30 values, which were higher than 90%, ensured good reliability and high quality of the sequencing data.

As shown in **Table 5**, at the kingdom level, the relative abundance of bacteria was, as expected, invariably much higher than archaea due to the strict requirement of the existence of environment for the latter. The relative abundances of bacteria in R′ at all the stages were higher than those in R. This confirmed again that THPT was capable of bettering the substrate nutrition and in turn boosted proliferation of bacteria. Accelerating growth of bacteria during continuous AD of TH tofu indeed accounted for the low VFA concentrations at the third stage (**Figure 4E**). Unfortunately, the relative abundance of archaea always remained at low levels (at a maximum value of ~0.1), confining AD of both the R and R′ groups. By contrast, the relative abundance of archaea (<0.02) was significantly lower in R′ than in R during continuous AD at high organic loads, suggesting that THPT of protein-rich tofu facilitated growth of more bacteria to bigger extents to suppress archaea and thus resulting in the final failure of AD of TH tofu.

(b) Bacterial community structure analysis

Figures 5A–D depict the recognized communities of bacterial domain at different taxonomic levels. At the phylum level, firmicutes, bacteroidetes, chloroflexi, synergistetes, patescibacteria, and cloacimonetes stood out in the community structure with the former three phyla dominating. These bacterial phyla were also found in various substrates of AD, for instance, in one-stage AD of pig slurry with fruit–vegetable waste (Ros et al., 2017) and other biogas reactors (Stets et al., 2014; Jabari et al., 2016) as well as in two-stage AD of abattoir wastewater, heterogeneous fruit–vegetable solid waste and their combinations (Hailu et al., 2021), though the phyla proteobacteria and firmicutes dominated in AD of the substrates not rich in proteins.

TABLE 4 | Statistics of sample bacteria sequencing data processing results and alpha diversity.

Classification	Sample ID	Clean total tags	Q30 (%)	GC (%)	OTUs	Simpson	Shannon	Chao1
Bacteria	R11	92,956	92.9	52.9	465	0.115	4.31	465.4
	R12	89,179	92.8	53.7	462	0.097	4.56	463
	R21	76,331	92.9	53.7	451	0.134	4.35	451.8
	R22	85,440	92.6	54.0	516	0.070	5.01	516.2
	R31	87,697	93.1	53.2	516	0.135	4.4	516.5
	R32	83,601	92.8	53.4	483	0.048	5.34	483.3

Note: GC, content, the ratio of guanine to cytosine; Q30, the percentage of bases with mass value >30 in the total base.

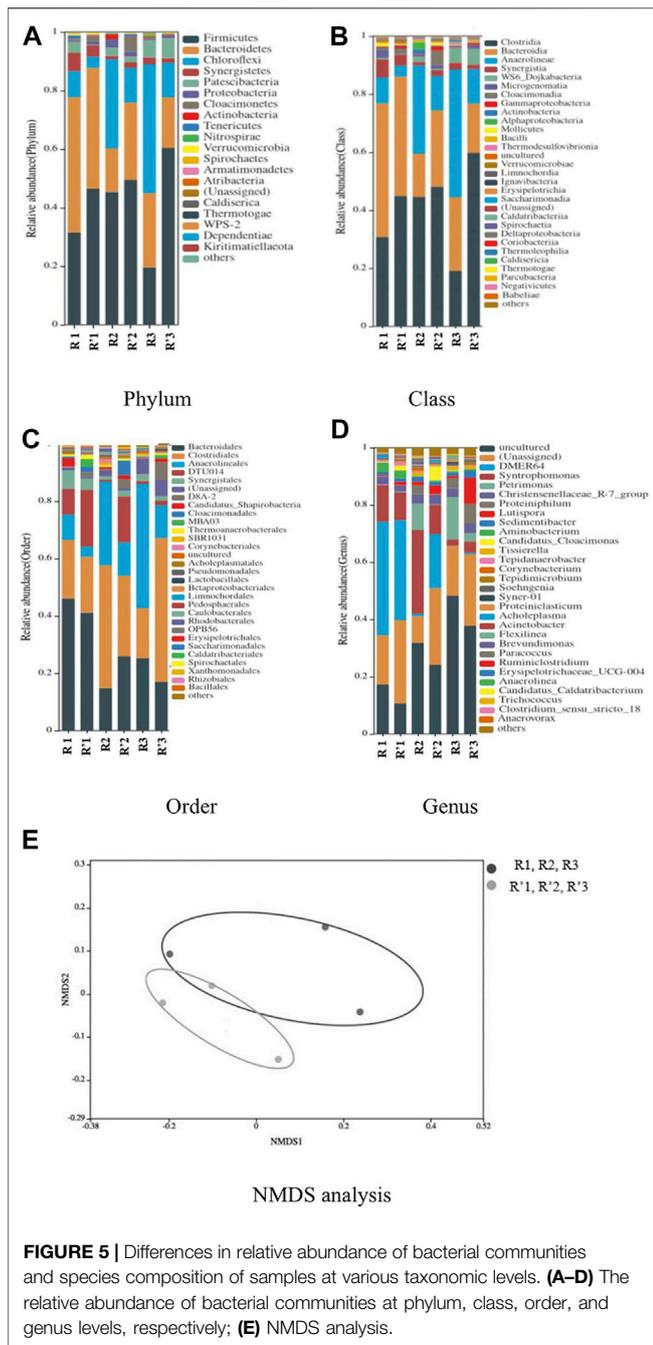**TABLE 5 |** Relative abundances of bacteria and archaea present during different AD stages at kingdom level.

Kingdom	R1	R′2	R2	R′2	R3	R′3
Bacteria	0.9951	0.9966	0.9656	0.9898	0.8966	0.9838
Archaea	0.0049	0.0034	0.0344	0.0102	0.1034	0.0162

Note: R/R′1–3 refer to the initial, second (stable), and last (final) stages during continuous AD, of tofu without and with THTP.

The two phyla of firmicutes and synergistetes are capable of degrading carbohydrates and proteins by hydrolases (Jang et al., 2015) and the bacteroidetes phylum frequently plays a key role in the hydrolysis process, and they surely contributed heavily to VFA production. According to Chen et al. (2018), the phylum firmicutes has a certain tolerance to high concentration TAN. While the phylum bacteroidetes decreased with heightened organic load of protein-rich tofu, firmicutes took on, as expected, an upward trend. Moreover, its relative abundance in R′ was always higher than that in R, indicating that the bacteria in the firmicutes phylum had better adaptabilities to TH tofu. Generally speaking, when being subjected to HTPT proteins, denaturation/degradation took place to certain degrees to form ammonia (and small molecule organic acids)/denatured proteins (Han et al., 2017). This actually confirmed that the firmicutes phylum is adaptive to AN as well as the worse nutrition (denatured proteins). However, for the chloroflexi phylum, which is responsible for digestion of organic compounds, oxidation of VFAs, and production of H_2 (Satoh et al., 2012), the reverse was true. This suggested that chloroflexi was not needed by TH Tofu at great quantities but the raw tofu, possibly because TH tofu could provide enough nutritious matter for microbes, which were produced by hydrolytic acidification microorganisms including chloroflexi. In addition to being capable of degrading carbohydrates by hydrolases to provide short-chain organic fatty acids (Jang et al., 2015), the phylum synergistetes can also use other organisms to decompose proteins and peptides to produce amino acids and sulfates for terminal metabolization of microbes such as methanogens and sulfate-reducing bacteria (Vartoukian et al., 2007). According to Luo et al. (2015), the phylum proteobacteria was the main consumer of propionate, butyrate, and acetate. Its relative abundance decreased significantly with the digestion proceeding, indicating that the degradation of VFAs became weaker at high ammonia nitrogen concentrations. The patescibacteria phylum, well-adaptive to

extreme environments (Tian et al., 2020), appeared at increasing relative abundances in the third stage of continuous AD (the organic load of protein-rich tofu being the highest). The phylum cloacimonetes has the ability to produce hydrogen in the acid production system of protein-rich substrates and usually cooperate closely with hydrogenotrophic methanogens by the synergistic symbiotic relationship, according to Saha et al. (2019). It appeared at an obvious abundance at the stable stage (the end of the first stage), especially in R′, though it almost disappeared completely at high organic loads. This augured that the hydrogenotrophic methanogenic pathway in the TH tofu would play a more important role in methanogenesis than in the raw tofu when there was no visible inhibition happening. Overall, TH of tofu facilitated growth of bacteria with better tolerance to ammonia.

As **Figure 5B** shows, bacteroidia, clostridia, and anaerolineae dominated at the class level. In light of the tofu substrate being rich in proteins, all the three dominant classes are, as expected, hydrogen-producing acetogenic bacteria, which could grow synergistically with hydrogenotrophic methanogens (Ziganshin et al., 2019). This confirmed the crucial function of the hydrogenotrophic methanogenesis pathway for AD of protein-rich tofu for biogas production. For the class bacteroidia (bacteroidea phylum), which can convert amino acids produced by protein hydrolysis into acetate (Ariesyady et al., 2007), its relative abundance continued to decrease with the AD proceeding from the most dominant position at the initial stage of digestion. As a member of the firmicutes phylum adaptive to high AN concentrations and denatured proteins as mentioned above, the class clostridia, which can convert organic matter into VFAs, mainly acetic acid and propionic acid (Feng et al., 2015; Sanz et al., 2017) and also convert amino acids into CO_2 and H_2 (Matteuzzi et al., 1978), gradually increased from the initial stage and become the most prominent at the stable stage regardless of THPT (R2 and R′2). However, increasing organic load of tofu resulted in decrease of its relative abundance (R′3), while the trend was reversed when tofu was subjected to THPT. This probably implied that HTPT of protein-rich substrate (here tofu) facilitated growth of ammonia-tolerant bacteria. For the anaerolineae class, acting on the degradation of protein and polysaccharide, their relative abundance increased all the time in R, but increased first and then remained stable in R′, basically consistent with the same trend for the chloroflexi phylum. With respect to the other main classes, synergistia (synergistetes

FIGURE 5 | Differences in relative abundance of bacterial communities and species composition of samples at various taxonomic levels. **(A–D)** The relative abundance of bacterial communities at phylum, class, order, and genus levels, respectively; **(E)** NMDS analysis.
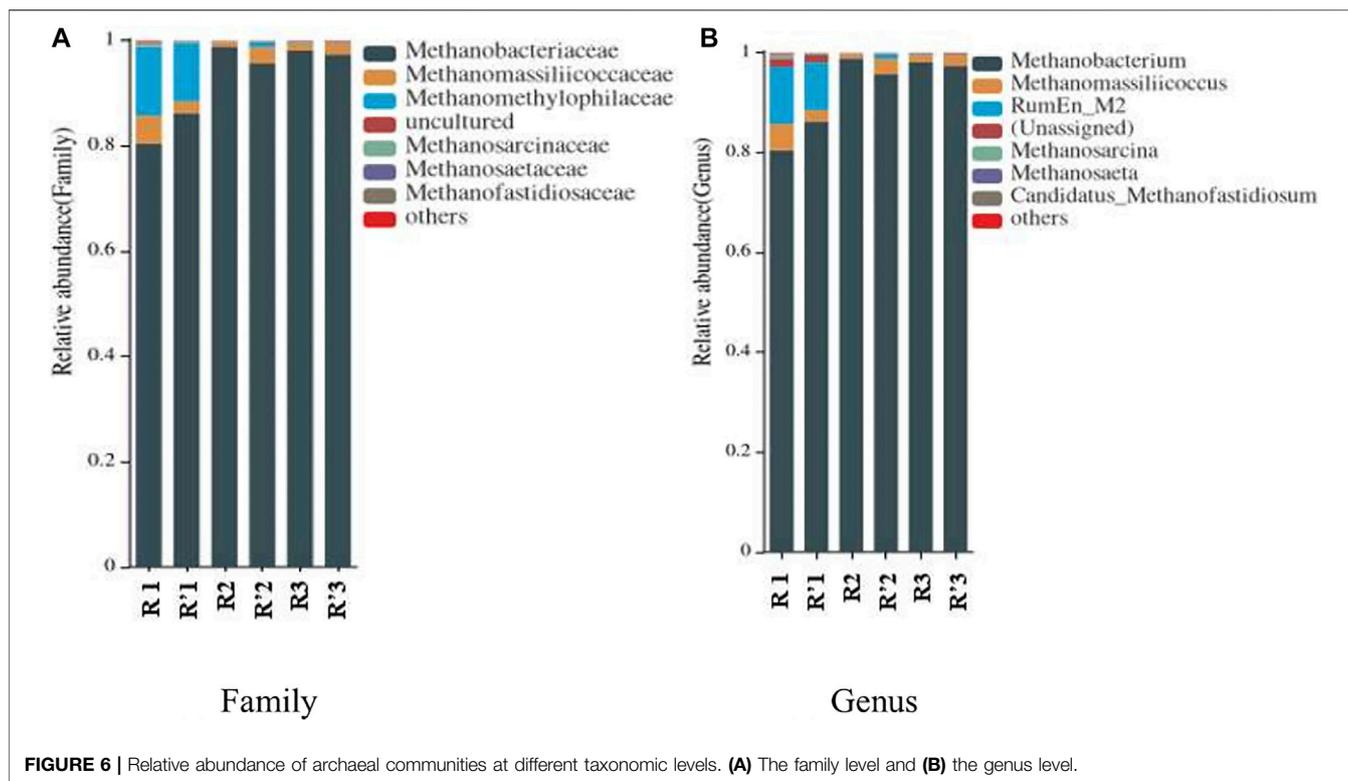
phylum), cloacimonadia (cloacimonetes phylum), and WS6_Dojkabacteria reached their peak abundances at the initial, stable, and last stages, respectively. Certain amounts of the class synergistia existed at the initial stage and it, as anticipated, decreased with increasing organic load of protein-rich tofu in light of its worse resistance to AN. By contrast, the class cloacimonadia, which can convert amino acids into CO_2 and H_2 and have also a symbiotic relationship with hydrogenotrophic methanogens just like anaerlineae and clostridia, appeared at the peak abundance at the stable stages of TH tofu. It was worth mentioning that visible amounts of WS6_Dojkabacteria, a

member of candidate bacterial phyla (CBP) in Candidate Phyla Radiation (CPR), reached the peak abundance at the last AD stage, indicating its strong resistance to extreme environmental conditions.

As presented in **Figure 5C**, the order *bacteroides*, which belongs to the hydrogen-producing acetogenic bacteria, dominated at the initial stage of digestion; however, its relative abundance decreased gradually. The clostridiales order was the main strain in R′ during ammonia inhibition, with its relative abundance accounting for 49.4%. The strictly anaerobic anaerolineales order can use a variety of substrates, such as sugar, peptides, and organic acids (Yamada et al., 2006). Its relative abundance kept increasing all the time in R and was invariably higher than that in R′. Particularly, the order synergistales, belonging to acetophilic bacteria, can perform mutual oxidation of acetic acid coupled with hydrogenotrophic methanogens. When the concentration of acetic acid was high, synergistales decomposed acetic acid together with the methanogens (methanosaeta, methanomicrobia class) (Ito et al., 2011). At the initial stage of digestion, the relative abundance of synergistales in R was higher than that in R′, which accorded with accumulation of acetic acid in the initial stage of R (refer to **Figure 4D**), appealing for synergistales to decompose acetic acid to produce CO_2 and H_2. Nonetheless, the order synergistales decreased because of its low growth speed (Ito et al., 2011). For the order clostridia D8A-2, which was found to have the potential to resist high ammonia concentrations similar to well-known SAOBs (Lee et al., 2019) and may fall within one new type of ammonia-tolerant SAOB, its relative abundance increased with the increase of ammonia concentration, especially in R′. The orders clostridia D8A-2 and clostridia DTU014 can be considered as potential co-cultured bacteria, and they can cooperate with methanogens to accelerate the methanogenic process of VFAs under ammonia stress. According to Lee et al. (2019), clostridia D8A-2 acts on acetic acid and clostridia DTU014 acts on propionic acid.

At the genus level, the two bacteria with constantly high relative abundances, dominating at the last stage, are uncultured or unassigned. Except for them, the genus rikenellaceae DMER64 was the prominent one followed by the genera syntrophomonas, petrimonas, christensenellaceae_R-7_group, and the like. The genera rikenellaceae DMER64 and christensenellaceae R-7 Group were identified as potential SAOBs, which can work together with methanosaeta concilii, methanineinacea, and methanobactins to degrade VFAs by methanogenesis. Though the relative abundances of the genera rikenellaceae DMER64 group and christensenellaceae R-7 group were found to increase significantly with the increase of ammonia concentration (Lee et al., 2019), in this research, the relative abundance of Rikenellaceae DMER64 decreased significantly, especially in R. This indeed meant that THPT relieved the inhibition effect of ammonia on the Rikenellaceae DMER64 to some degree, therefore implying that the THPT group produced more methane through the SAO–HM pathway. The syntrophomonas genus is a typical butyric acid degrading bacterial one capable of converting butyric acid into acetic acid. At the stable stage of continuous AD of the raw tofu

FIGURE 6 | Relative abundance of archaeal communities at different taxonomic levels. **(A)** The family level and **(B)** the genus level.

(R2), its relative abundance in the untreated group was higher than that in the THPT group, according to the fact that there was more butyric acid accumulation in the untreatment group. The genus petrimonas can degrade carbohydrates into hydrogen and acetate (Lei et al., 2018). In R, its relative abundance increased remarkably and reached the highest value and became dominant under the condition of ammonia inhibition taking place, while only slightly increased in R′, possibly because it could not be accustomed to the TH tofu substrate.

The NMDS analysis of bacteria in the samples was performed, and the results are shown in **Figure 5E**, which are used to compare the differences between/among the sample groups, based on sample information contained in the species and using form of points on the multidimensional space. As **Figure 5E** depicts, the spatial distance between the anchor points for different samples in R′ is shorter compared to those in R, indicating that the composition structure of species in R′ was more similar to each other than in R. Furthermore, this meant that the bacterial community structure changed to relatively smaller degrees and the digestion system was more stable.

(c) Archaeal community structure analysis

Various methanogenic archaea are included in the phylum euryarchaeota (Sorokin et al., 2017). In this research, the classes methanobacteria, methanomicrobia, and thermoplasmata were detected with methanobacteria dominating, and at the order level, methanobacteriales occupied the overwhelming proportion, followed by methanomassiliicoccales and other orders

(including methanosarcinales, methanomicrobiales, and methanofastidiosales) with their relative abundances significantly decreasing (data not given here). **Figure 6** gives the relative abundance of archaeal communities at different taxonomic levels. It can be clearly seen from **Figure 6A** that, at the family level, there dominated methanosaetaceae (methanosarcinales order), which can utilize hydrogen, formic acid, methanol, methyl amine, and acetic acid as the substrates to generate methane. The relative abundance of the family methanomethylophilaceae (methanomassiliicoccales order) was just second to the methanosaetaceae family. Generally, strictly H_2-dependent methylotrophic methanogens are the members of methanomethylophilaceae. The family methanosarcinaceae, and particularly methanosarcina spp., are versatile, which can perform methylotrophic, aceticlastic, and hydrogenotrophic methanogenesis. The members of the methanosaetaceae family are known as acetate-consuming microorganisms, which are slow-growing and show a low minimum threshold for acetate. The classes methanosaetaceae and methanosarcinaceae (both belonging to the methanosarcinales order) and the order methanobacteriales were negatively correlated with the TAN concentration, conductivity, and potassium concentration of liquid digestate, but positively correlated with the pH and free ammonia concentration of liquid digestate, while the opposite was the case for the methanomicrobiales. The total relative abundances of methanosaetaceae, methanosarcinaceae, and methanobacteriales were positively correlated with methane production, while that of methanomicrobiales was negatively correlated with methane production. The order

methanomassiliicoccales was the seventh group of methanogens found in a variety of anaerobic environments, including the gastrointestinal tract of humans and other animals and are considered to be essential hydrogen-dependent methylotrophic methanogens. The order methanofastidiosales falls within hydrogen-dependent methylotrophic methanogens, similar to methanomassiliicoccales (Borrel et al., 2014; Söllinger and Urich, 2019). Overall, there were more hydrogenotrophic methanogens in R, but part of them were replaced by methylotrophic and aceticlastic methanogens in R'.

As **Figure 6B** shows, at the genus level, hydrogenotrophic methanobacterium (methanosaetaceae family) had the highest relative abundance. Following methanobacterium, the genus RumEnM2, which belongs to the methanomethylophilaceae family and is a new methyl methanogenic genus that has not been reported, existed at the stable stage of AD of TH of tofu (R'2), though it remarkably decreased from the initial stage. The genus methanomassiliicoccus, which belongs to the methanomassiliicoccaceae family (methanomassiliicoccales order), was the third rich and also appeared at higher relative abundances at the stable (R'2) and later (R'3) stages in the THPT group. That is, relatively more methylotrophic and aceticlastic methanogens were present at the middle and late stages of AD of TH tofu compared to that of the raw tofu. This supported the methylotrophic pathways for THPT of protein-rich substrates (here tofu), and at the same time accounted for relatively higher biogas yields for TH tofu than the raw tofu as well. Furthermore, more aceticlastic methanogens could account to some degree for the slow response of the HT tofu acclimated AD process to the change of organic load.

4 CONCLUSION

For AD of protein-rich tofu with increasing organic load, the inhibition by acidification prior to accumulation of AN occurred. THPT helped overcome the acidification inhibition present in

batch AD of tofu at such a high TS content of 3.6%, to obtain the maximum methane yield rate of 589.39 ml·(gVS)$^{-1}$. In the continuous AD, ammonia-tolerant bacteria and hydrogenotrophic methanogens played crucial roles. The continuous AD processes acclimated by HT protein-rich substrates seemed to be resistant to severe organic loads, by boosting growth of ammonia-tolerant microorganisms, above all methylotrophic methanogens such as the genera RumEnM2 and methanomassiliicoccus. Nevertheless, the process of continuous AD of HT protein-rich substrates responded belatedly to change of organic loads approaching the upper limitation value, meaning that a sufficiently long adaptation period was necessary to stabilize the AD system.

DATA AVAILABILITY STATEMENT

The datasets presented in this study can be found in online repositories. The names of the repository/repositories and accession number(s) can be found at: https://www.ncbi.nlm.nih.gov/, BioProject ID: PRJNA779218.

AUTHOR CONTRIBUTIONS

The first two authors contribute to the work equally and mutually finished most of the research work and this paper. The middle three authors carried out some experiments, and the last two authors gave some suggestions about the related experiment design and paper writing.

REFERENCES

Akiya, N., and Savage, P. E. (2002). Roles of Water for Chemical Reactions in High-Temperature Water. *Chem. Rev.* 102 (8), 2725–2750. doi:10.1021/cr000668w

Appels, L., Baeyens, J., Degrève, J., and Dewil, R. (2008). Principles and Potential of the Anaerobic Digestion of Waste-Activated Sludge. *Prog. Energ. Combust. Sci.* 34 (6), 755–781. doi:10.1016/j.pecs.2008.06.002

Ariesyady, H. D., Ito, T., and Okabe, S. (2007). Functional Bacterial and Archaeal Community Structures of Major Trophic Groups in a Full-Scale Anaerobic Sludge Digester. *Water Res.* 41 (7), 1554–1568. doi:10.1016/j.watres.2006.12.036

Borrel, G., Gaci, N., Peyret, P., O'Toole, P. W., Gribaldo, S., and Brugère, J.-F. (2014). Unique Characteristics of the Pyrrolysine System in the 7th Order of Methanogens: Implications for the Evolution of a Genetic Code Expansion Cassette. *Archaea* 2014 (1), 1–11. doi:10.1155/2014/374146

Bougrier, C., Delgenès, J. P., and Carrère, H. (2008). Effects of thermal Treatments on Five Different Waste Activated Sludge Samples Solubilisation, Physical Properties and Anaerobic Digestion. *Chem. Eng. J.* 139 (2), 236–244. doi:10.1016/j.cej.2007.07.099

Boulanger, A., Pinet, E., Bouix, M., Bouchez, T., and Mansour, A. A. (2012). Effect of Inoculum to Substrate Ratio (I/S) on Municipal Solid Waste Anaerobic Degradation Kinetics and Potential. *Waste Manage.* 32, 2258–2265. doi:10.1016/j.wasman.2012.07.024

Calli, B., Mertoglu, B., Inanc, B., and Yenigun, O. (2005). Community Changes during Start-Up in Methanogenic Bioreactors Exposed to Increasing Levels of Ammonia. *Environ. Techn.* 26 (1), 85–91. doi:10.1080/09593332608618585

Chen, S., He, J., Wang, H., Dong, B., Li, N., and Dai, X. (2018). Microbial Responses and Metabolic Pathways Reveal the Recovery Mechanism of an Anaerobic Digestion System Subjected to Progressive Inhibition by Ammonia. *Chem. Eng. J.* 350, 312–323. doi:10.1016/j.cej.2018.05.168

Chukwu, O., and Ismail, D. A. (2010). Effect of Hydrothermal Treatments on Proteins from Acha (Digitaria Exilis) and Wheat (Triticum Durum). *As. J. Food Ag-Ind.* 2, 93–101.

D'Abzac, P., Bordas, F., Hullebusch, E. V., Lens, P. N. L., and Guibaud, G. (2010). Extraction of Extracellular Polymeric Substances (EPS) from Anaerobic Granular Sludges: Comparison of Chemical and Physical Extraction Protocols. *Appl. Microbiol. Biotechnol.* 85, 1589–1599. doi:10.1007/s00253-009-2288-x

Dorn-In, S., Gareis, M., and Schwaiger, K. (2019). Differentiation of Live and Dead *Mycobacterium tuberculosis* Complex in Meat Samples Using PMA qPCR. *Food Microbiol.* 84, 103275–103283. doi:10.1016/j.fm.2019.103275

Eaton, A. (2005). *Standard Methods for the Examination of Water and Wastewater.* Washington DC: APHA, American Public Health Association.

Feng, Y., Zhang, Y., Chen, S., and Quan, X. (2015). Enhanced Production of Methane from Waste Activated Sludge by the Combination of High-Solid Anaerobic Digestion and Microbial Electrolysis Cell with Iron-Graphite Electrode. *Chem. Eng. J.* 259, 787–794. doi:10.1016/j.cej.2014.08.048

Franke-Whittle, I. H., Walter, A., Ebner, C., and Insam, H. (2014). Investigation into the Effect of High Concentrations of Volatile Fatty Acids in Anaerobic Digestion on Methanogenic Communities. *Waste Manage.* 34 (11), 2080–2089. doi:10.1016/j.wasman.2014.07.020

Hailu, A. M., Palani, S. G., Asfaw, S. L., and Tegaye, T. A. (2021). Insight into Microbial Community Diversity and Composition of Two-Stage Anaerobic Digestion: Focusing Methanogenic Stage. *Bioresour. Techn. Rep.* 15, 100764. doi:10.1016/j.biteb.2021.100764

Han, W., Fotidis, I. A., and Irini, A. (2015). Ammonia Effect on Hydrogenotrophic Methanogens and Syntrophic Acetate-Oxidizing Bacteria. *FEMS Microbiol. Ecol.* 91 (11), 130. doi:10.1093/femsec/fiv130

Han, Y., Zhuo, Y., Peng, D., Yao, Q., Li, H., and Qu, Q. (2017). Influence of thermal Hydrolysis Pretreatment on Organic Transformation Characteristics of High Solid Anaerobic Digestion. *Bioresour. Techn.* 244, 836–843. doi:10.1016/j.biortech.2017.07.166

Harris, P. W., Schmidt, T., and Mccabe, B. K. (2017). Evaluation of Chemical, Thermobaric and Thermochemical Pre-treatment on Anaerobic Digestion of High-Fat Cattle Slaughterhouse Waste. *Bioresour. Techn.* 244, 605–610. doi:10.1016/j.biortech.2017.07.179

Hobson, P. N., and Shaw, B. G. (1976). Inhibition of Methane Production by Methanobacterium Formicicum. *Water Res.* 10 (10), 849–852. doi:10.1016/0043-1354(76)90018-x

Ito, T., Yoshiguchi, K., Ariesyady, H. D., and Okabe, S. (2011). Identification of a Novel Acetate-Utilizing Bacterium Belonging to Synergistes Group 4 in Anaerobic Digester Sludge. *ISME J.* 5, 1844–1856. doi:10.1038/ismej.2011.59

Jabari, L., Gannoun, H., Khelifi, E., Cayol, J. L., Godon, J. J., Hamdi, M., et al. (2016). Bacterial Ecology of Abattoir Wastewater Treated by an Anaerobic Digestor. *Braz. J. Microbiol.* 47 (1), 73–84. doi:10.1016/j.bjm.2015.11.029

Jang, H. M., Ha, J. H., Park, J. M., Kim, M.-S., and Sommer, S. G. (2015). Comprehensive Microbial Analysis of Combined Mesophilic Anaerobic-Thermophilic Aerobic Process Treating High-Strength Food Wastewater. *Water Res.* 73, 291–303. doi:10.1016/j.watres.2015.01.038

Jia, X., Xi, B., Li, M., Liu, D., Hou, J., Hao, Y., et al. (2017). Metaproteomic Analysis of the Relationship between Microbial Community Phylogeny, Function and Metabolic Activity during Biohydrogen-Methane Coproduction under Short-Term Hydrothermal Pretreatment from Food Waste. *Bioresour. Techn.* 245, 1030–1039. doi:10.1016/j.biortech.2017.08.180

Kim, M.-J., and Kim, S.-H. (2020). Conditions of Lag-phase Reduction during Anaerobic Digestion of Protein for High-Efficiency Biogas Production. *Biomass Bioenergy* 143 (2), 105813. doi:10.1016/j.biombioe.2020.105813

Kim, D., Lee, K., and Park, K. Y. (2015). Enhancement of Biogas Production from Anaerobic Digestion of Waste Activated Sludge by Hydrothermal Pre-treatment. *Int. Biodeterioration Biodegradation* 101, 42–46. doi:10.1016/j.ibiod.2015.03.025

Koster, I. W. (2010). Characteristics of the pH-Influenced Adaptation of Methanogenic Sludge to Ammonium Toxicity. *J. Chem. Technol. Biot.* 36 (10), 445–455. doi:10.1002/jctb.280361003

Kruse, A., and Dinjus, E. (2007). Hot Compressed Water as Reaction Medium and Reactant. *J. Supercrit. Fluids* 39, 362–380. doi:10.1016/j.supflu.2006.03.016

Lee, J., Koo, T., Yulisa, A., and Hwang, S. (2019). Magnetite as an Enhancer in Methanogenic Degradation of Volatile Fatty Acids under Ammonia-Stressed Condition. *J. Environ. Manage.* 241, 418–426. doi:10.1016/j.jenvman.2019.04.038

Lei, Y., Wei, L., Liu, T., Xiao, Y., Dang, Y., Sun, D., et al. (2018). Magnetite Enhances Anaerobic Digestion and Methanogenesis of Fresh Leachate from a Municipal Solid Waste Incineration Plant. *Chem. Eng. J.* 348, 992–999. doi:10.1016/j.cej.2018.05.060

Li, D., Tong, T., Zeng, S., Lin, Y., Wu, S., and He, M. (2014). Quantification of Viable Bacteria in Wastewater Treatment Plants by Using Propidium Monoazide Combined with Quantitative PCR (PMA-qPCR). *J. Environ. Sci.* 26 (2), 299–306. doi:10.1016/s1001-0742(13)60425-8

Li, N., Xue, Y., Chen, S., Takahashi, J., Dai, L., and Dai, X. (2017). Methanogenic Population Dynamics Regulated by Bacterial Community Responses to Protein-Rich Organic Wastes in a High Solid Anaerobic Digester. *Chem. Eng. J.* 317, 444–453. doi:10.1016/j.cej.2017.02.098

Lissens, G., Thomsen, A. B., De Baere, L., Verstraete, W., and Ahring, B. K. (2004). Thermal Wet Oxidation Improves Anaerobic Biodegradability of Raw and Digested Biowaste. *Environ. Sci. Technol.* 38 (12), 3418–3424. doi:10.1021/es035092h

Liu, X., Du, M., Yang, J., Wu, Y., Xu, Q., Wang, D., et al. (2020). Sulfite Serving as a Pretreatment Method for Alkaline Fermentation to Enhance Short-Chain Fatty Acid Production from Waste Activated Sludge. *Chem. Eng. J.* 385, 123991. doi:10.1016/j.cej.2019.123991

Liu, J., Yin, J., He, X., Chen, T., and Shen, D. (2021a). Optimizing Food Waste Hydrothermal Parameters to Reduce Maillard Reaction and Increase Volatile Fatty Acid Production. *J. Environ. Sci.* 103, 43–49. doi:10.1016/j.jes.2020.09.032

Liu, X., Wu, Y., Xu, Q., Du, M., Wang, D., Yang, Q., et al. (2021b). Mechanistic Insights into the Effect of Poly Ferric Sulfate on Anaerobic Digestion of Waste Activated Sludge. *Water Res.* 189, 116645. doi:10.1016/j.watres.2020.116645

Luo, J., Feng, L., Chen, Y., Sun, H., Shen, Q., Li, X., et al. (2015). Alkyl Polyglucose Enhancing Propionic Acid Enriched Short-Chain Fatty Acids Production during Anaerobic Treatment of Waste Activated Sludge and Mechanisms. *Water Res.* 73, 332–341. doi:10.1016/j.watres.2015.01.041

Massé, D., Masse, L., and Croteau, F. (2003). The Effect of Temperature Fluctuations on Psychrophilic Anaerobic Sequencing Batch Reactors Treating Swine Manure. *Bioresour. Techn.* 89 (1), 57–62. doi:10.1016/s0960-8524(03)00009-9

Mateo-Sagasta, J., Raschid-Sally, L., and Thebo, A. (2015). "Global Wastewater and Sludge Production, Treatment and Use," in *Wastewater*. Editors P. Drechsel, M. Qadir, and D. Wichelns (Dordrecht: Springer), 15–38. doi:10.1007/978-94-017-9545-6_2

Matteuzzi, D., Crociani, F., and Emaldi, O. (1978). Amino Acids Produced by Bifidobacteria and Some Clostridia. *Ann. Microbiol.* 129b, 175–181.

Nimas, M. S., SunyotoZhu, M., Zhang, Z., and Zhang, D. (2017). Effect of Biochar Addition and Initial pH on Hydrogen Production from the First Phase of Two-phase Anaerobic Digestion of Carbohydrates. *Food Waste. Energ. Proced.* 105, 379–384. doi:10.1115/1.4039318

Ramsay, I. R., and Pullammanappallil, P. C. (2001). Protein Degradation during Anaerobic Wastewater Treatment: Derivation of Stoichiometry. *Biodegradation* 12, 247–256. doi:10.1023/a:1013116728817

Resch, C., Wörl, A., Waltenberger, R., Braun, R., and Kirchmayr, R. (2011). Enhancement Options for the Utilisation of Nitrogen Rich Animal By-Products in Anaerobic Digestion. *Bioresour. Techn.* 102 (3), 2503–2510. doi:10.1016/j.biortech.2010.11.044

Ros, M., de Souza Oliveira Filho, J., Perez Murcia, M. D., Bustamante, M. A., Moral, R., Coll, M. D., et al. (2017). Mesophilic Anaerobic Digestion of Pig Slurry and Fruit and Vegetable Waste: Dissection of the Microbial Community Structure. *J. Clean. Prod.* 156 (10), 757–765. doi:10.1016/j.jclepro.2017.04.110

Saha, S., Jeon, B.-H., Kurade, M. B., Chatterjee, P. K., Chang, S. W., Markkandan, K., et al. (2019). Microbial Acclimatization to Lipidic-Waste Facilitates the Efficacy of Acidogenic Fermentation. *Chem. Eng. J.* 358, 188–196. doi:10.1016/j.cej.2018.09.220

Sanz, J. L., Rojas, P., Morato, A., Mendez, L., Ballesteros, M., and González-Fernández, C. (2017). Microbial Communities of Biomethanization Digesters Fed with Raw and Heat Pre-treated Microalgae Biomasses. *Chemosphere* 168, 1013–1021. doi:10.1016/j.chemosphere.2016.10.109

Satoh, H., Tsushima, I., Miura, Y., Ito, T., and Okabe, S. (2012). Characterization of Microbial Community Structures and Their Activities in Single Anaerobic Granules by Beta Imaging, Microsensors and Fluorescence *In Situ* Hybridization. *Water Sci. Technol.* 65 (12), 2125–2131. doi:10.2166/wst.2012.117

Siegert, I., and Banks, C. (2005). The Effect of Volatile Fatty Acid Additions on the Anaerobic Digestion of Cellulose and Glucose in Batch Reactors. *Process Biochem.* 40 (11), 3412–3418. doi:10.1016/j.procbio.2005.01.025

Söllinger, A., and Urich, T. (2019). Methylotrophic Methanogens Everywhere - Physiology and Ecology of Novel Players in Global Methane Cycling. *Biochem. Soc. T.* 47, 1895–1907. doi:10.1042/bst20180565

Sorokin, D. Y., Makarova, K. S., Abbas, B., Ferrer, M., Golyshin, P. N., Galinski, E. A., et al. (2017). Discovery of Extremely Halophilic, Methyl-Reducing Euryarchaea Provides Insights into the Evolutionary Origin of Methanogenesis. *Nat. Microbiol.* 2 (8), 17081–17111. doi:10.1038/nmicrobiol.2017.81

Stets, M. I., Etto, R. M., Galvão, C. W., Ayub, R. A., Cruz, L. M., Steffens, M. B. R., et al. (2014). Microbial Community and Performance of Slaughterhouse Wastewater Treatment Filters. *Genet. Mol. Res.* 13 (2), 4444–4455. doi:10.4238/2014.june.16.3

Tian, R., Ning, D., He, Z., Zhang, P., Spencer, S. J., Gao, S., et al. (2020). Small and Mighty: Adaptation of Superphylum Patescibacteria to Groundwater Environment Drives Their Genome Simplicity. *Microbiome* 8 (1), 51–15. doi:10.1186/s40168-020-00825-w

Tyagi, V. K., Bhatia, A., Kubota, K., Rajpal, A., Ahmed, B., Khan, A. A., et al. (2021). Microbial Community Dynamics in Anaerobic Digesters Treating Organic Fraction of Municipal Solid Waste. *Environ. Techn. Innovation* 21 (3-4), 101303. doi:10.1016/j.eti.2020.101303

Vartoukian, S. R., Palmer, R. M., and Wade, W. G. (2007). The Division "Synergistes". *Anaerobe* 13 (3-4), 99–106. doi:10.1016/j.anaerobe.2007.05.004

Venkiteshwaran, K., Bocher, B., Maki, J., and Zitomer, D. (2015). Relating Anaerobic Digestion Microbial Community and Process Function. *Microbiol. Insights* 8, 37–44. doi:10.4137/MBI.S33593

Villamil, J. A., Mohedano, A. F., San Martín, J., Rodriguez, J. J., and de la Rubia, M. A. (2020). Anaerobic Co-digestion of the Process Water from Waste Activated Sludge Hydrothermally Treated with Primary Sewage Sludge. A New Approach for Sewage Sludge Management. *Renew. Energ.* 146, 435–443. doi:10.1016/j.renene.2019.06.138

Wang, Y., Zhang, Y., Wang, J., and Meng, L. (2009). Effects of Volatile Fatty Acid Concentrations on Methane Yield and Methanogenic Bacteria. *Biomass Bioenergy* 33 (5), 848–853. doi:10.1016/j.biombioe.2009.01.007

Wang, T., Zhai, Y., Zhu, Y., Peng, C., Xu, B., Wang, T., et al. (2018). Influence of Temperature on Nitrogen Fate during Hydrothermal Carbonization of Food Waste. *Bioresour. Techn.* 247, 182–189. doi:10.1016/j.biortech.2017.09.076

Xue, Y., Liu, H., Chen, S., Dichtl, N., Dai, X., and Li, N. (2015). Effects of thermal Hydrolysis on Organic Matter Solubilization and Anaerobic Digestion of High Solid Sludge. *Chem. Eng. J.* 264, 174–180. doi:10.1016/j.cej.2014.11.005

Yamada, T., Sekiguchi, Y., Hanada, S., Imachi, H., Ohashi, A., Harada, H., et al. (2006). Anaerolinea Thermolimosa Sp. nov., Levilinea Saccharolytica Gen. nov., Sp. Nov. And Leptolinea Tardivitalis Gen. nov., Sp. nov., Novel Filamentous Anaerobes, and Description of the New Classes Anaerolineae Classis Nov. and Caldilineae Classis Nov. In the Bacterial Phylum Chloroflexi. *Int. J. Syst. Evol. Microbiol.* 56 (6), 1331–1340. doi:10.1099/ijs.0.64169-0

Yang, L., Huang, Y., Zhao, M., Huang, Z., Miao, H., Xu, Z., et al. (2015). Enhancing Biogas Generation Performance from Food Wastes by High-Solids Thermophilic Anaerobic Digestion: Effect of pH Adjustment. *Int. Biodeterioration Biodegradation* 105, 153–159. doi:10.1016/j.ibiod.2015.09.005

Chen, Y., Cheng, J. J., and Creamer, K. S. (2008). Inhibition of Anaerobic Digestion Process: a Review. *Bioresour. Technol.* 99 (10), 4044–4064. doi:10.1016/j.biortech.2007.01.057

Zeng, S., Yuan, X., Shi, X., and Qiu, Y. (2010). Effect of Inoculum/substrate Ratio on Methane Yield and Orthophosphate Release from Anaerobic Digestion of Microcystis Spp. *J. Hazard. Mater.* 178, 89–93. doi:10.1016/j.jhazmat.2010.01.047

Zhang, G., Ma, D., Peng, C., Liu, X., and Xu, G. (2014). Process Characteristics of Hydrothermal Treatment of Antibiotic Residue for Solid Biofuel. *Chem. Eng. J.* 252, 230–238. doi:10.1016/j.cej.2014.04.092

Zhang, G., Li, C., Ma, D., Zhang, Z., and Xu, G. (2015). Anaerobic Digestion of Antibiotic Residue in Combination with Hydrothermal Pretreatment for Biogas. *Bioresour. Techn.* 192, 257–265. doi:10.1016/j.biortech.2015.05.014

Zhang, W., Li, L., Xing, W., Chen, B., Zhang, L., Li, A., et al. (2019). Dynamic Behaviors of Batch Anaerobic Systems of Food Waste for Methane Production under Different Organic Loads, Substrate to Inoculum Ratios and Initial pH. *J. Biosci. Bioeng.* 128 (6), 733–743. doi:10.1016/j.jbiosc.2019.05.013

Zhu, Q., Liu, S., Gao, P., and Luan, F. (2014). High-throughput Sequencing Technology and its Application. *J. Northeast Agric. Univ.* 21 (3), 84–96. doi:10.1016/S1006-8104(14)60073-8

Ziganshin, A. M., Wintsche, B., Seifert, J., Carstensen, M., Born, J., and Kleinsteuber, S. (2019). Spatial Separation of Metabolic Stages in a Tube Anaerobic Baffled Reactor: Reactor Performance and Microbial Community Dynamics. *Appl. Microbiol. Biotechnol.* 103, 3915–3929. doi:10.1007/s00253-019-09767-2